The Atmospheric Surface Layer as a Model for Canonical Turbulent Boundary Layers

Beverley McKeon
Graduate Aerospace Laboratories
California Institute of Technology
http://mckeon.caltech.edu

Motivation: high Reynolds number boundary layers

Industrial piping	$Re_D > 10^7$	$D^+ > 10^5$
Boeing 777 fuselage	$Re_x > 10^8$	
Boeing 777 wing	$Re_x > 10^7$	
Near-neutral ASL	?	$\delta^+ \sim 10^6$

- Fundamentally important study of the behavior of "very high Reynolds number" wall-bounded flow with direct implications for industrial-/transport-scale flows (simulations are not predictive – experiments for input to models)
- Evaluation of the *near-neutrally stable* atmospheric surface layer as a model for the canonical zero pressure gradient turbulent boundary layer in the highest available Reynolds number terrestrial boundary layer test facility
- Experimental pros/cons
  - Easing of resolution constraints usually associated with high Reynolds number
  - Non-stationarity of the surface layer flow

Outline

- Why use the planetary boundary layer to advance fundamental studies of canonical wall turbulence?
- Brief description of the general atmospheric boundary layer
- Experimental concerns in the atmospheric surface layer
- The near-neutral atmospheric surface layer as a model for the canonical turbulent boundary layer
- Results from the near-neutral atmospheric surface layer: which questions can we tackle?

Who else studies the ASL?

- Micrometeorologists
  - wind flow near the ground
- Meteorologists
  - weather (synoptic weather systems, local storms)
  - aeronautical meteorology (low level clouds, jets, etc)
  - agricultural meteorology (dew, frost etc)

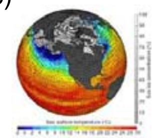

- Climate dynamicists
  - clouds, fluxes, gaseous exchange etc.
  - global circulation (GCMs need influence of boundary)
- Researchers in convective and stably stratified flow
- Urban planners, structural engineers (wind loading)
- Environmental engineers
  - air pollution
  - pollutant dispersion)

The planetary boundary layer

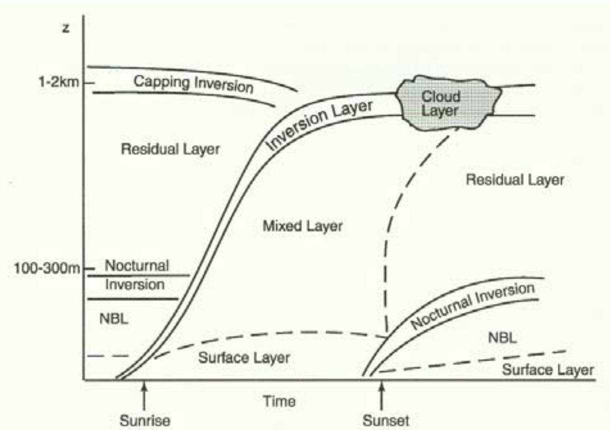

Convectively-driven Stably stratified

Near-neutral Near-neutral

Wyngaard, Annu. Rev. Fluid Mech. (1992)

- Incompressible
- Huge range of scales
- Coriolis force
  - dependence of the results on latitude, wind direction…
  - but not in the surface layer
- Different relative importance of mechanical shear and thermal effects on atmospheric turbulence
- Top boundary condition important
  - heat transfer can generate stable/unstable stratification
  - e.g. clouds, entrainment of less-dense air)

Stable boundary layer

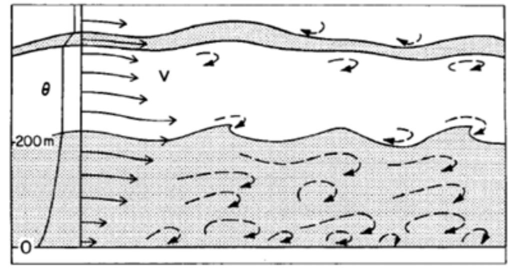

Wyngaard, Annu. Rev. Fluid Mech. (1992)

- E.g. night time state under clear skies
- Turbulence production only from mean wind shear
- Radiative cooling of the surface leads to positive vertical gradient of potential temperature and buoyancy force that counters vertical displacement
- Only eddies with inertial forces at least as large as this buoyancy force are observed, i.e. $l_{\max} \sim \left(\dfrac{q^2}{\beta\theta_3}\right)^{1/2}$

Atmospheric Surface Layer (ASL)

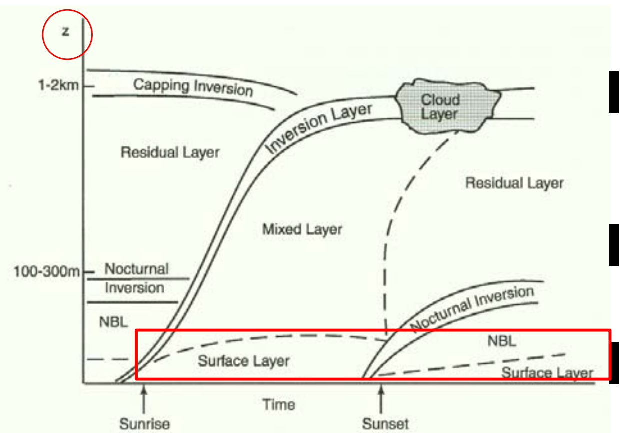

Convectively-driven Stably stratified

Near-neutral Near-neutral

Wyngaard, Annu. Rev. Fluid Mech. (1992)

- Bottom ~10% of planetary boundary layer
- Depth varies with the diurnal cycle (resets at sunrise and sunset)
- “Constant stress”: fluxes close to surface values
- Near-neutral/neutral: mechanical shear-driven flow

Convective boundary layer

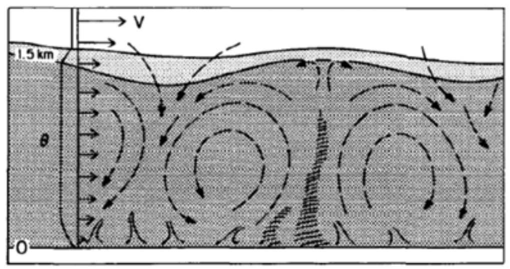

Wyngaard, Annu. Rev. Fluid Mech. (1992)

- Common day-time state over land (also over the sea)
- Driven by surface temperature flux (plus moisture flux)
- Surface layer, mixed layer, interfacial layer
- Turbulent Coriolis forces usually negligible (large Rossby number)
- Surface heating and evaporation drives convective layer to first inversion
- (Mean wind shear may play a role)

Quantification of buoyancy effects

- Turbulent Kinetic Energy equation for horizontally homogeneous flow

$$\frac{\partial e}{dt} = -\overline{u'w'}\frac{\partial U}{dz} - \overline{v'w'}\frac{\partial V}{dz} + \left(\frac{g}{\theta_v}\right)\overline{w'\theta'_v} - \frac{\partial}{dz}\left(\overline{w'e} + \frac{\overline{w'p'}}{\rho}\right) - \varepsilon = 0$$

- Virtual potential temperature θ_v
  - treat moist air as a perfect gas with a gas constant of dry air but a virtual temperature which the dry air would have to have to achieve the actual density at the actual pressure (T_v)
  - bring air to STP adiabatically (θ_v)

$$\theta_v = T_v\left(\frac{P_0}{P}\right)^{R_d/C_{Pd}}$$

- Production for $d\theta_v/dz < 0$ and vice versa (truly neutral flow rare for entire ASL)
- For low humidity in the ASL, $\theta_v \sim T_v \sim T$

Equipment: general

- Remote, e.g. sodar, acoustic radar, lidar, Doppler radar (spatial volume averages)
- Mini-SODAR
  - Sound Detection and Ranging
  - Speed of sound ~340 m/s cf $3\text{x}10^8$m/s for radio
  - 3 antennae for 3 velocity components
- Balloons, tethersonde
- Planes
  - Mobility, load capacity
  - Extended line traverses in x, z (80 m/s)
  - BUT need to quantify plane motion accurately
- Etc

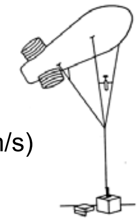

Monin-Obukhov theory

- Consider the height at which the production from buoyancy and shear are equal, i.e.

$$-\overline{u'w'}\frac{\partial U}{\partial z} = \left(\frac{g}{\theta_v}\right)\overline{w'\theta_v}$$

- Define L, the Monin-Obukhov length as the height at which these terms are equal

$$L = \frac{-u_\tau^3}{\kappa(g/\overline{\theta_v})\overline{w'\theta_v}}$$

- Approximate neutral stability for $|z/L| << 1$
  - $|z/L|<<0.1$ (Hogstrom et al)
  - $|z/L|<0.01$ (Brasseur et al)

Equipment: specific

- Cup and vane anemometer

- Sonic anemometer

- Constant temperature anemometry
  - Single hot-wires
  - X-wires
  - Multi-wire probes
- Flow visualization (smoke, etc)
- Particle image velocimetry
- Surface pressure measurements

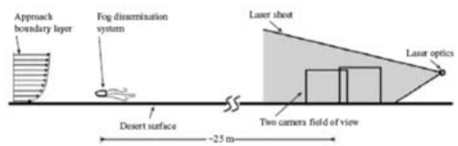

- … etc…*"Large-scale" vs "small-scale" information*

The near-neutral ASL as a model for the canonical ZPG boundary layer

- Mean wind shear generates turbulent kinetic energy
- δ_s from minimum of gradient of horizontal velocity profile

ADVANTAGES
- Highest terrestrial Reynolds numbers
- Large physical and temporal scales
- “Free”!

DISADVANTAGES
- Buoyancy effects
- Upper boundary condition
- Wall boundary condition
- Uncontrolled
  - Wind velocity
  - Wind direction
  - Temperature
- Field campaigns difficult
- Weather…

Determination of skin friction

Three main methods
- Direct: drag plate
- I[redacted]direct:
  - Velocity gradient near the wall
- I[redacted]direct:
  - Measurement of shear stress in the constant stress region

Large error bars, but “reasonable” agreement between methods

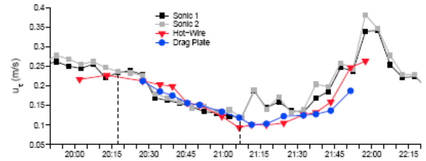

M.Metzger, PhD thesis (2002)

Surface roughness

- Roughness influence traditionally determined by introducing aerodynamic roughness length z_0

$$U^+ = \frac{1}{\kappa}\ln\frac{z-d}{z_0}$$

- z_0 corresponds to the z location where an extrapolated log law reaches zero velocity
- SLTEST/salt flats: roughness heights k ~1-5mm, z_0 ~ 10^{-5}m
- Sample values of z_0 given on the right
  - h_c canopy height
  - d zero plane displacement (level of action of drag on roughness elements)

Table A6. *Values of aerodynamic roughness length and zero-plane displacement for a range of natural surfaces*

Surface	Reference	h_c (m)	z_0 (m)	d/h_c
soils			0.001–0.01	
grass				
thick	Sutton (1953)	0.1	0.023	
thin	Sutton (1953)	0.5	0.05	
sparse	Clarke *et al.* (1971)	0.025	0.0012	
	Deacon (1953)	0.015	0.002	
		0.45	0.018	
		0.65	0.039	
crops				
wheat stubble	Izumi (1971)	0.18	0.025	
wheat	Garratt (1977b)	0.25	0.005	
		0.4	0.015	
		1.0	0.05	
corn	Kung (1961)	0.8	0.064	
beans	Thom (1971)	1.18	0.077	
vines	Hicks (1973)	0.9	0.023[a]	
		1.4	0.12[b]	
vegetation	Fichtl and McVehil (1970)	1–2	0.2	
woodland				
trees	Fichtl and McVehil (1970)	10–15	0.4	
savannah	Garratt (1980)	8	0.4	0.6
		9.5	0.9	0.75
forests				
pine	Hicks *et al.* (1975)	12.4	0.32	
pine	Thom *et al.* (1975)	13.3	0.55	
		15.8	0.92	
coniferous	Jarvis *et al.* (1976)	10.4[c]–27.5	0.28–3.9	0.61–0.92
tropical	Thomson and Pinker (1975)	32	4.8	
tropical	Shuttleworth (1989)	35	2.2	0.85

[a] Flow parallel to rows.
[b] Flow normal to rows.
[c] Range in h_c for 11 sites; the mean z_0/h_c is 0.076 and the mean d/h_c is 0.78.

J.R. Garratt: The Atmospheric Boundary Layer Cambridge

Stability

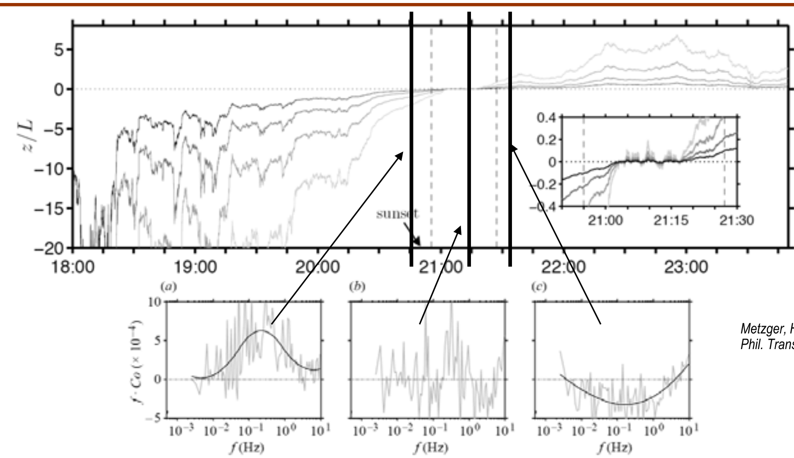

Metzger, Holmes & McKeon, Phil. Trans. Royal Soc. A 2007.

- Linear variation with time – “near-neutral transition period”
- |z/L| < 0.1 denoted by dashed lines “near-neutral period” (Hogstrom)
- |z/L| << 0.1 for data considered here
- L essentially constant with z in this regime

Problems associated with non-stationarity

- Mean conditions changing with timescale t_{bl}
- Largest eddies of turbulence have timescale t_t
- Must have $t_t << t_{bl}$ for quasi-steady flow
- However there may still be problems with convergence (depends on the location of the Panofsky gap with respect to t_t to some degree
  - Lumley convergence criterion

$$\sigma^2 = \left[\frac{1}{T}\int_0^T f(t+t')dt' - \overline{f(t)} \right]^2 \to 0 \qquad T \to \infty$$

$$\sigma^2 = \frac{2\overline{f'^2}}{T}\int_0^T \left(1 - \frac{t}{T}\right)\rho(t)dt \to 0$$

ρ is the autocorrelation with integral ζ, the integral lengthscale.

- Also need to consider where fixed probes are in non-dimensional space

Wind speed and direction

- Mean conditions changing (magnitude and direction)
- Neutral period not known a priori!

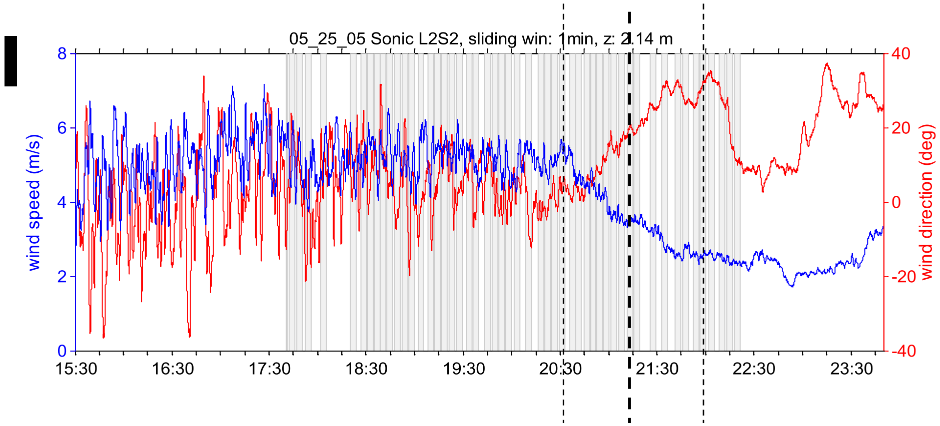

"Turbulence" vs "atmospheric motions"

- Consider planetary boundary layer:
  - Three-dimensional turbulence (cf intermittent turbulence due to instabilities, wind shear, cloud condensation…)
  - Non-stationarity of the flow
  - Continuous spectrum of atmospheric motions
  - Turbulence kinetic energy production associated with mean wind shear, change in terrain or surface roughness, presence of clouds, buoyancy…
- Statistical separation of turbulence requires a gap in the spectrum between different types of fluctuations
  - the "Panofsky gap"

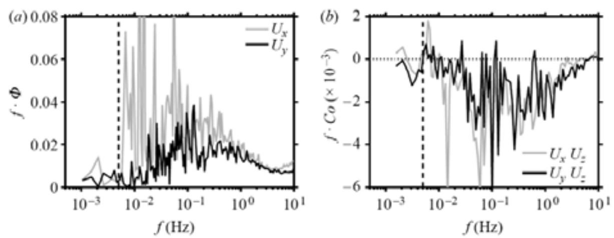

Metzger, Holmes & McKeon, Phil. Trans. Royal Soc. A 2007.

Averaging times vs sample frequency

- Sonic anemometers:
  - relatively low sampling frequencies (e.g.Campbell Scientific CSAT3, f_{sample}= 20Hz)
  - large spatial measurement volumes (~10cm^3)
  - long temporal records

CTA: higher frequencies, smaller measuring volumes but shorter sample periods

Convergence – major issue

Non-dimensional probe location?

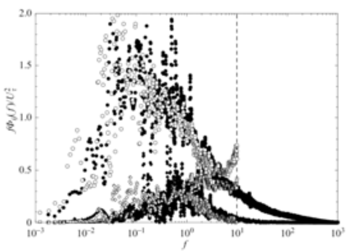

Kunkel & Marusic, J. Fluid Mech. 2006

Notable previous studies of the neutral ASL

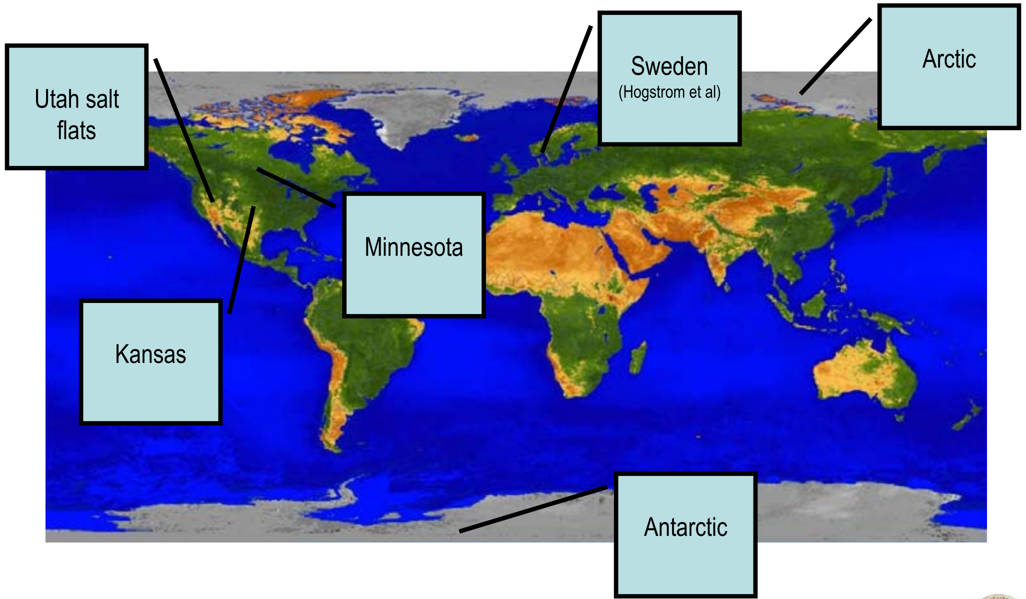

Images of SLTEST

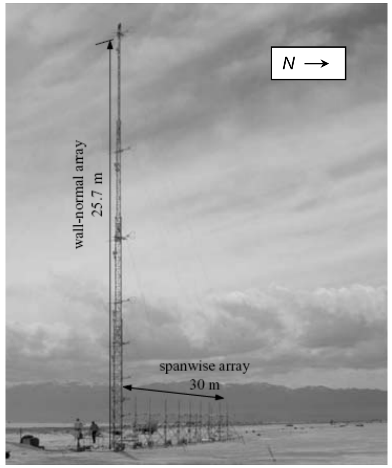

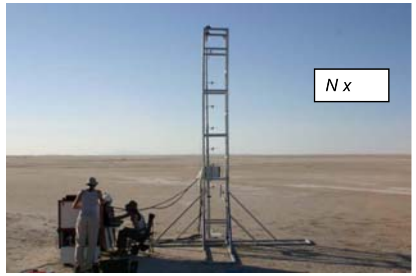

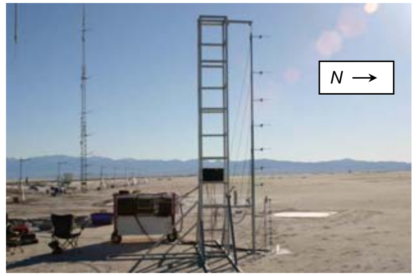

Surface Layer Turbulence and Environmental Science Test Facility (SLTEST)

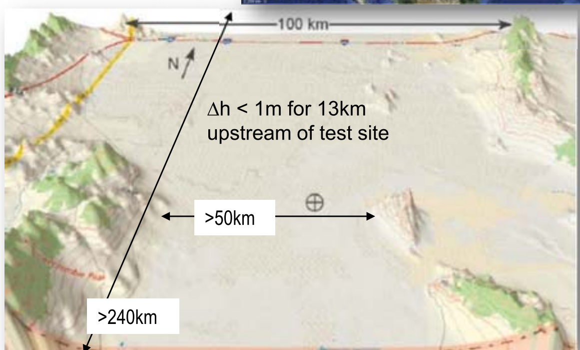

- Salt playa > 240km x 50km
- Δh < 1m for 13km upstream of test site
- 100km fetch to test site
- Predominantly northerly winds

Experimental considerations at SLTEST

- $|z/L| << 0.1$
- $U_{5m} \approx 5$ m/s
  $\delta \approx$ 50-100m
  $\delta^+ = \delta u_\tau/\nu \approx O(10^6)$
  $z_0 \sim 0.2$mm

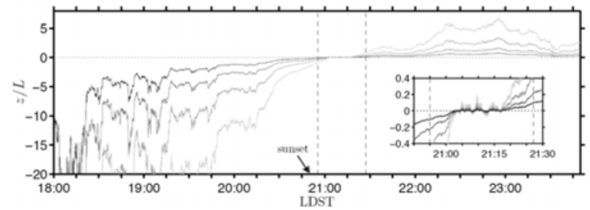

- Synchronous measurements at 31 log-spaced wall-normal locations
  - 5kHz sample frequency
  - T = 210s
  - $T^+ \sim 3 \times 10^5$, $TU_{5m}/\delta \sim 20$
- Friction velocity from sonic anemometer array (Campbell Scientific CSAT3, f_{sample}= 20Hz)

Metzger, Holmes & McKeon, Phil. Trans. Royal Soc. A 2007

Time dependence of the streamwise velocity

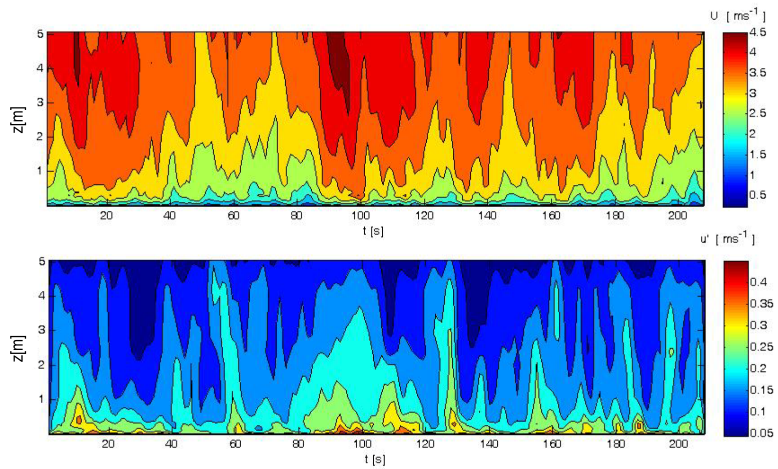

Guala, Metzger & McKeon, Phys. D, to appear

Influence of (in)stability

Andreas et al J. Fluid Mech. 2006

- Surface HEat Budget of the Arctic ocean (SHEBA)

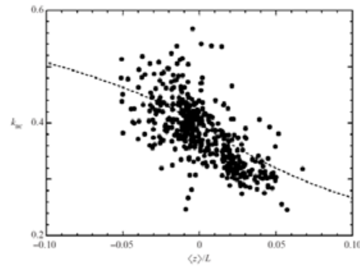

FIGURE 6. The uncorrected SHEBA k values as a function of the stratification, where $\langle z \rangle$ is the geometric mean of the five measurement heights and L is the median value of the five measured Obukhov lengths. The line is (5.2).

Mean velocity

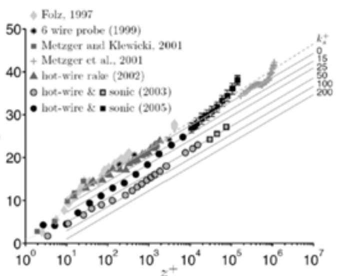

Metzger, Holmes & McKeon, Phil. Trans. Royal Soc. A 2007.

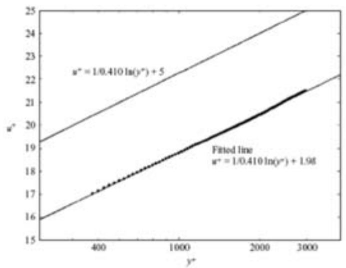

Morris et al J. Fluid Mech. 2007

- Span range of roughness from smooth to fully-rough
- Uncertainty in u_τ, non-stationarity, etc make scaling arguments extremely difficult (Nagib et al, 2007) estimate that <0.1% accuracy on C_f required)
- Behavior “logarithmic”

Spectra (u,w)

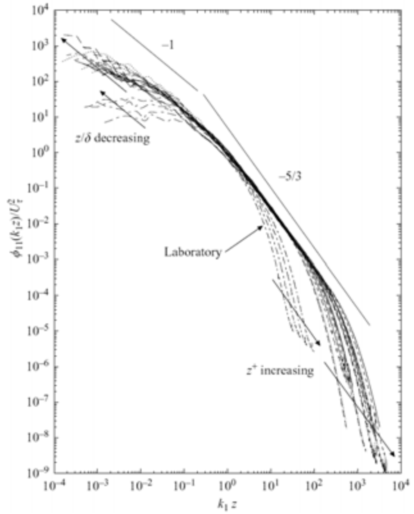

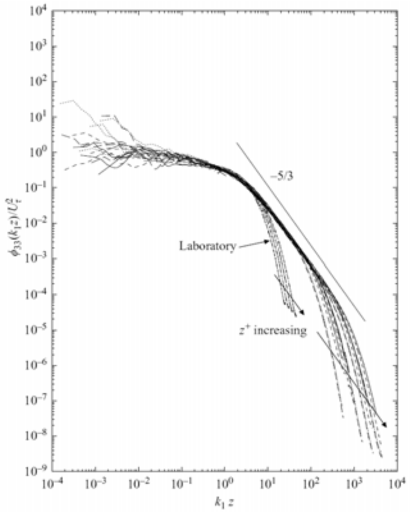

Kunkel & Marusic, J. Fluid Mech. 2006

Turbulent fluctuations (u)

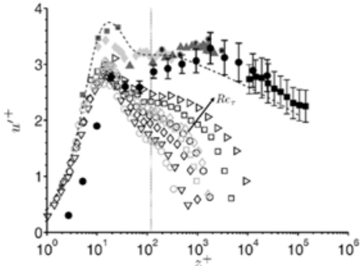

Metzger, Holmes & McKeon, Phil. Trans. Royal Soc. A 2007

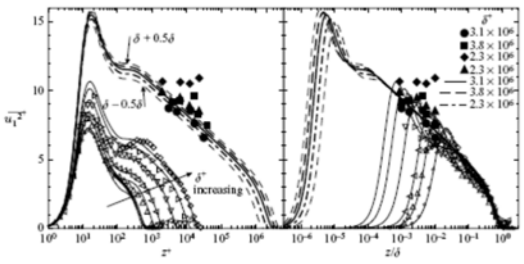

Kunkel & Marusic, J. Fluid Mech. 2006

- Clear influence of roughness sublayer (~ 3 x k_s^+)
- Evidence that near wall peak in streamwise turbulence intensity continues to grow with Reynolds number
  - Logarithmic dependence, per attached eddy model?

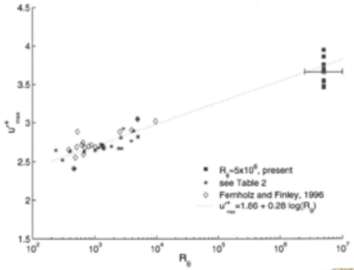

Metzger & Klewicki, Phys. Fluids 2001

Streamwise energy spectra

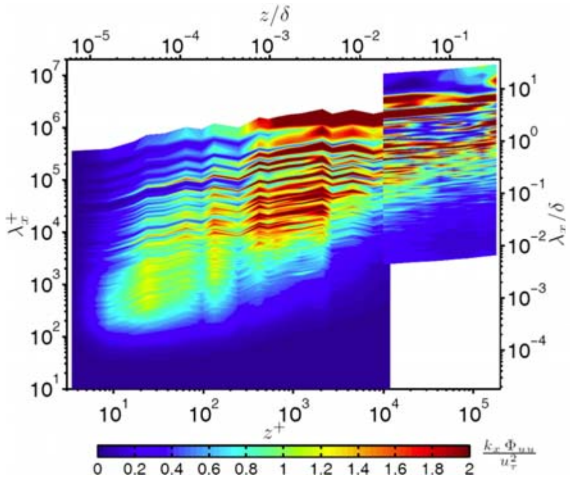

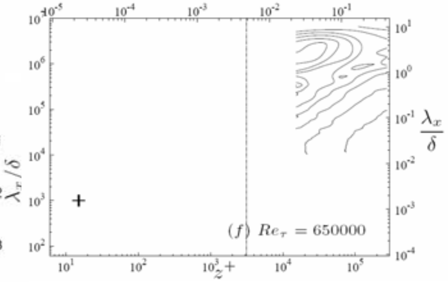

Mathis, Hutchins & Marusic, J. Fluid Mech. 2009

- SLTEST spectrum similar to $\delta^+ \sim 7300$ results of Hutchins & Marusic, 2007

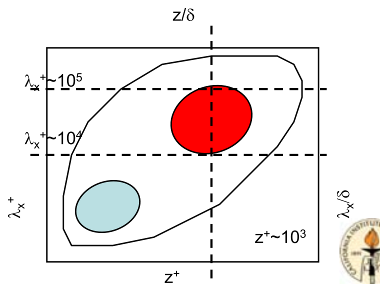

Turbulent fluctuations (w)

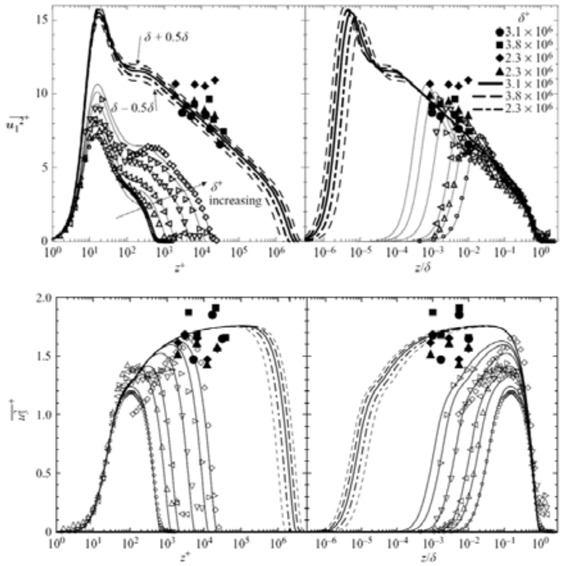

Kunkel & Marusic, J. Fluid Mech. 2006

Approach to local isotropy?

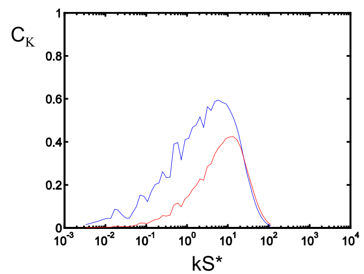

$y^+ = 480$

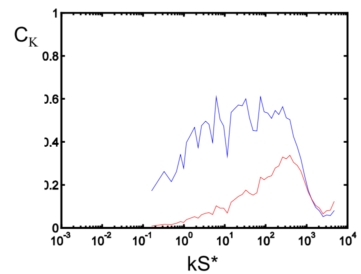

$y^+ = 36000$

- $k^{-5/3}$ compensated spectra at different wall-normal locations
- A self-similar 5/3rds plateau only emerges for high enough $y^+ \sim 1000$
- Overlap of the energy-containing and dissipation scales for $y^+ = 480$ where the local Reynolds number is too low for “strong” turbulence

Temporal and structural interpretations

Large-Scale Motions O(1-10δ)

Kim & Adrian, Morrison *et al*, Marusic *et al*

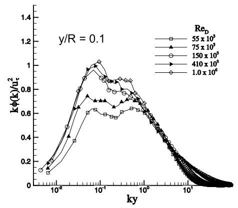

Uniform momentum zones & hairpin packet model

Adrian, Meinhart & Tomkins, J. Fluid Mech. 2000

Modulating/envelope effect on small-scales

Hutchins & Marusic, PTRSA 2007

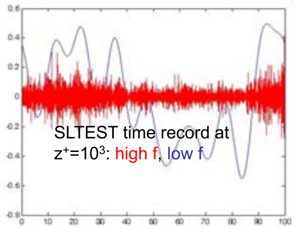

No hairpins?

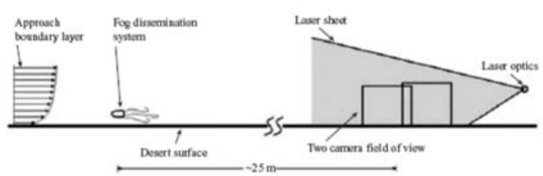

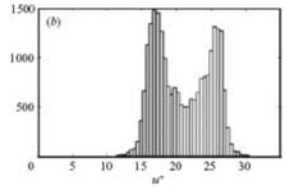

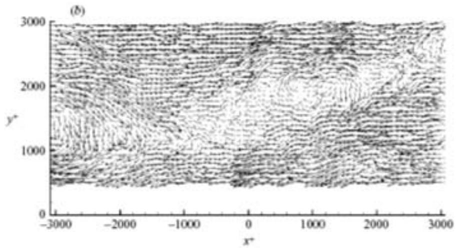

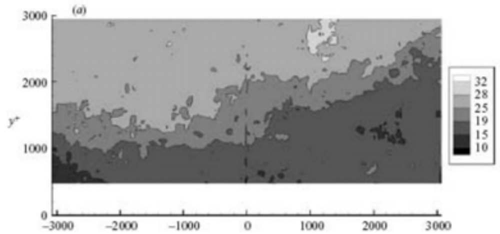

Morris et al J Fluid Mech. (2007)

Evidence of shear layers

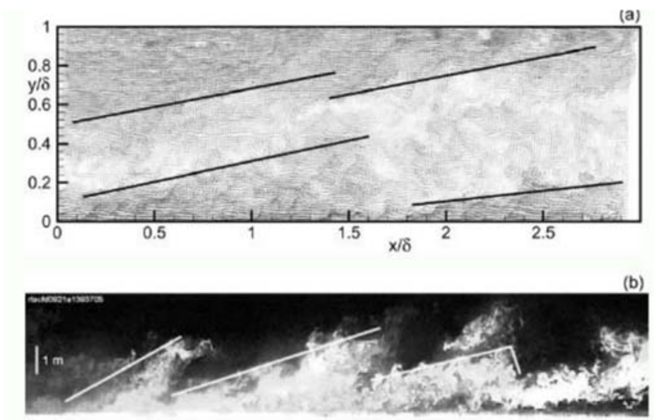

Figure 10. (a) PIV realization in the streamwise–wall-normal plane of a zero-pressure-gradient turbulent boundary layer at $Re_\theta = 7705$ (AMT). Note that the entire boundary layer is shown ($0 < x/\delta < 3$, $0 < y/\delta < 1$). (b) Smoke visualization of the wall-region ($0 < x/\delta < 0.01$, $0 < y/\delta < 0.015$) of the atmospheric boundary layer at $Re_\theta = 9 \times 10^6$. In both cases, air flow is from left to right. A constant convection velocity of $0.79U_\infty$ has been subtracted from the vectors in (a). A hierarchy of ramp-like structures with similar orientation and structure is observed in both figures. The approximate extent of these structures has been indicated with solid lines.

Hommema & Adrian, B. Layer Met. 2003

Composite streamwise velocity field

PIV field of view of Morris et al (2007)

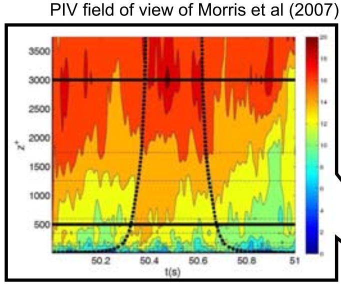

0.05 < z < 0.48m, x=2m

Temporal-to-spatial conversion from Taylor's hypothesis

Spatial equivalent would be R-L flow

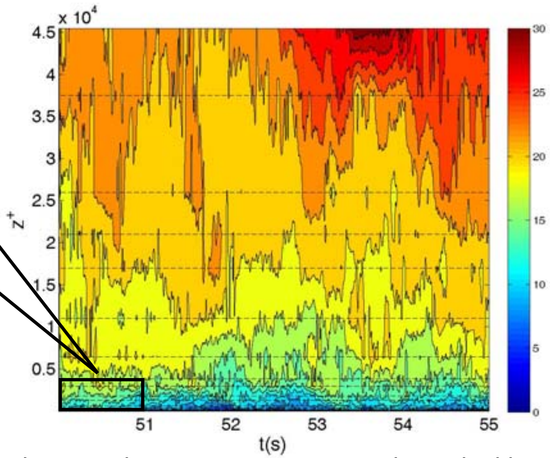

Sample composite of time-synchronous instantaneous streamwise velocities (actual probe locations denoted by horizontal dashed lines).

Contours calculated using an interpolated regularly spaced contour grid, transformed back to approx. logarithmic y spacing.

Instantaneous velocity profiles

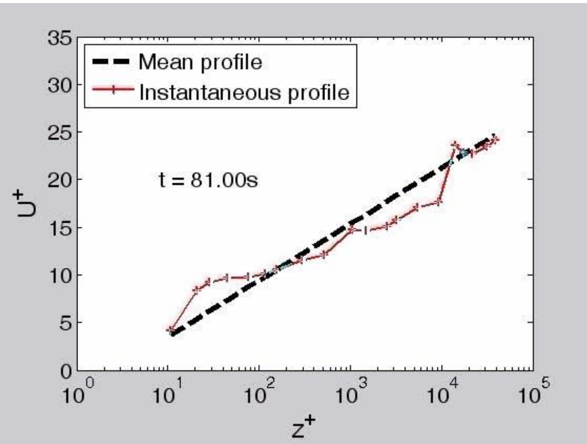

Sample instantaneous profiles

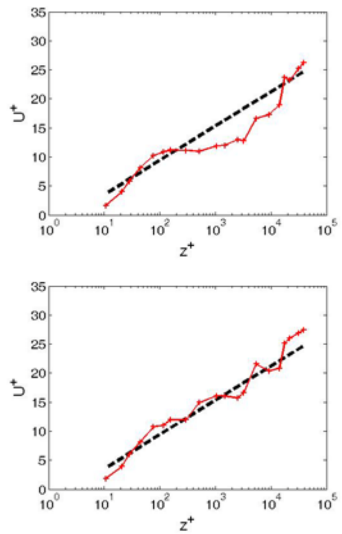

Wall-normal variation of modulating effect

Magnitude of amplitude modulation changes with wall-normal distance

- Bandyopadhyay & Hussain (1987)
- Mathis et al (2009)

$$R = \frac{\overline{u_L^+ E_L^+}}{\sqrt{\overline{u_L^{+2}}}\sqrt{\overline{E_L^{+2}}}}$$

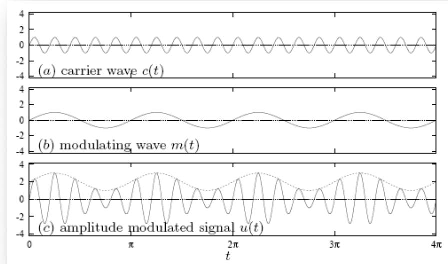

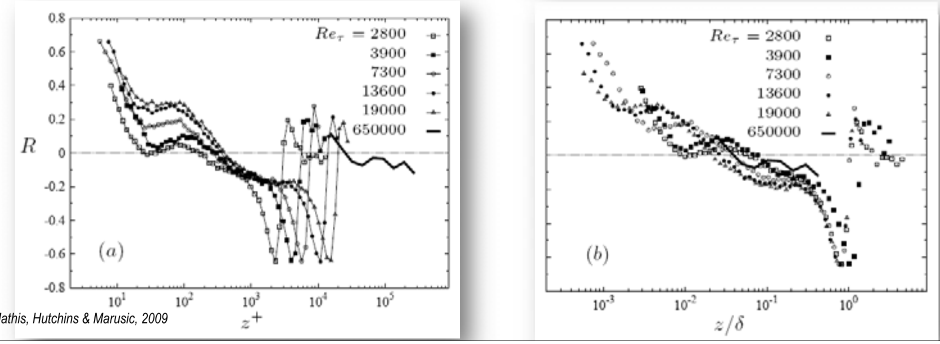

Mathis, Hutchins & Marusic, 2009

Influence of the large scales

- Composite fields confirm long temporal extent of uniform momentum zones
- Indication of spatial (wall-normal) and temporal alignment of these zones, confirmed by spectra of the streamwise fluctuations
- "Modulating" effect of the largest scales on the small-scale turbulence across the field of view

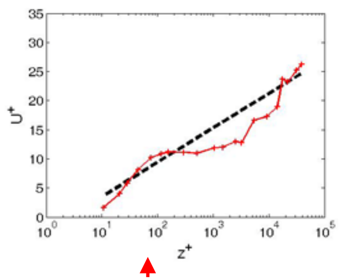

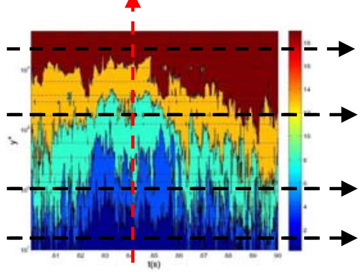

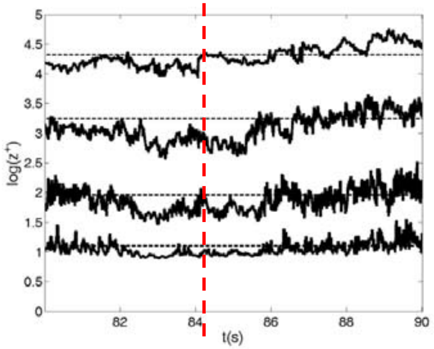

A hierarchy of scale modulation…

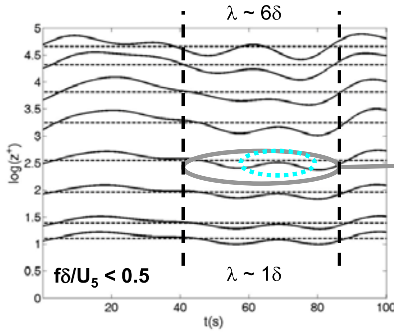

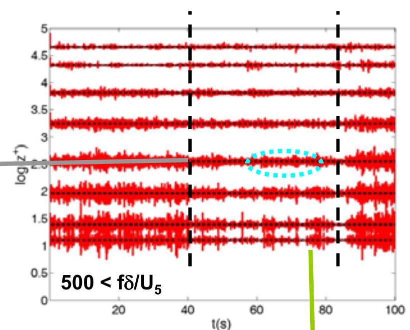

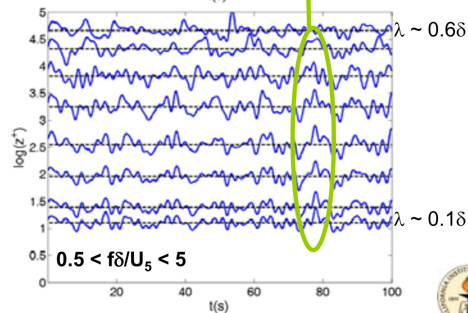

Frequency filters employed across the entire wall-normal data set (to permit constant convection velocities)

Negative excursions at a range of large scales are reflected in the small-scale intensities

Indications of "phase relationship" across scales

… down to the dissipative scales

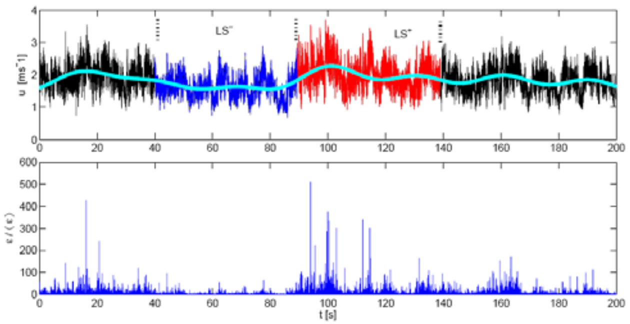

Intermittency of the dissipation signal also strongly affected by the large scales

Guala, Metzger & McKeon, Phys. D, to appear

Two-point correlations

Consider the two-point correlation with two reference z^+ locations

$$\rho_{uu}(r_x^+, z^+, z_{ref}^+) = \frac{\Sigma_x u(x, z_{ref}) u(x + r_x, z)}{\sqrt{\Sigma_x u^2(x, z_{ref})}\sqrt{\Sigma_x u^2(x, z)}}$$

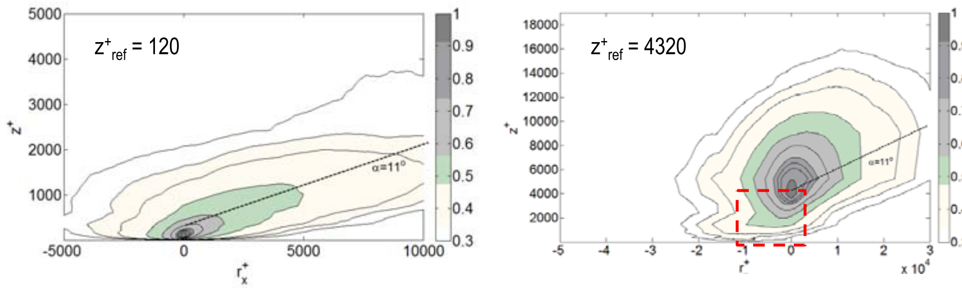

Guala, McKeon & Metzger, submitted

Spectral localization of the modulation effect

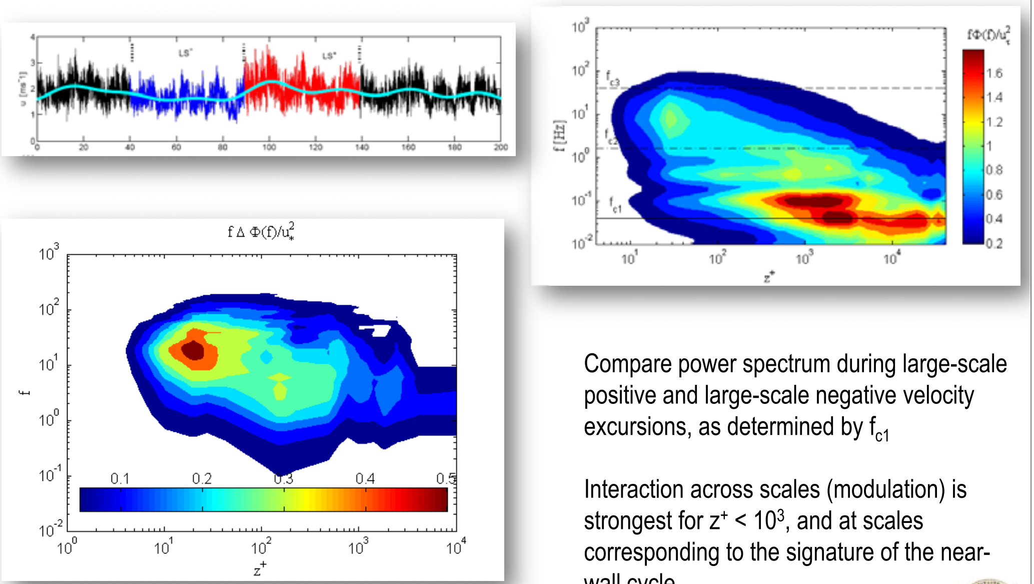

Compare power spectrum during large-scale positive and large-scale negative velocity excursions, as determined by f_{c1}

Interaction across scales (modulation) is strongest for $z^+ < 10^3$, and at scales corresponding to the signature of the near-wall cycle

Guala, McKeon & Metzger, submitted

Structure inclination angle

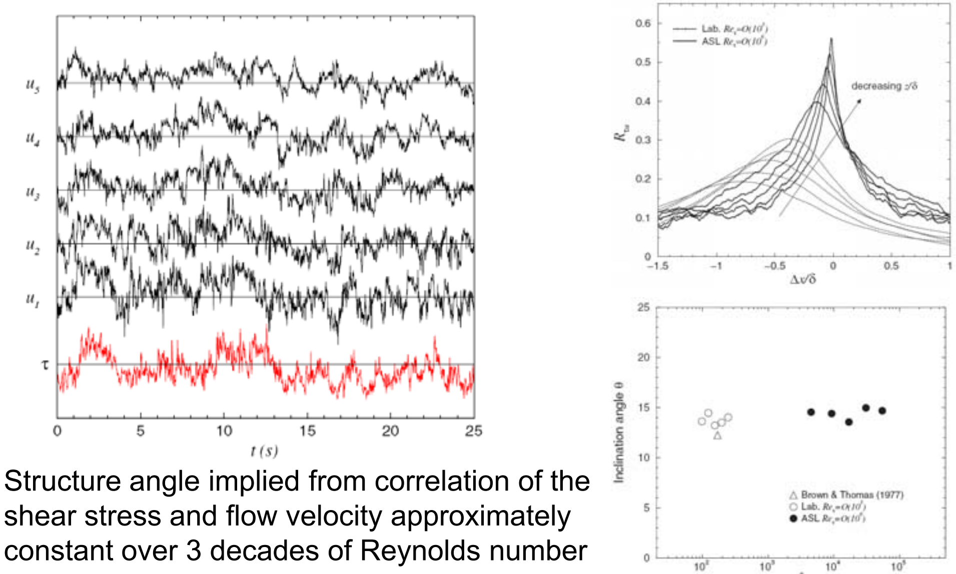

Structure angle implied from correlation of the shear stress and flow velocity approximately constant over 3 decades of Reynolds number

Marusic & Heuer, Phys. Rev. Letters, 2007

Evidence of superstructures

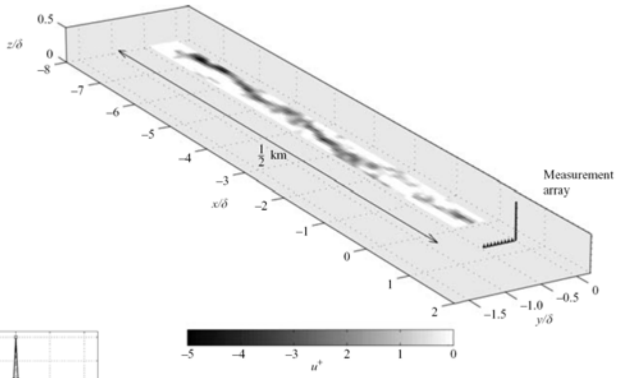

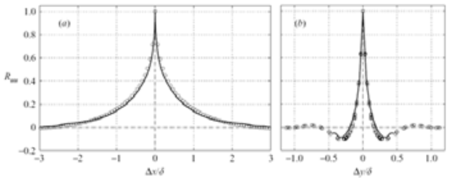

Hutchins & Marusic, J. Fluid Mech., 2007

Above: 100s reconstruction (~500m length).

Symbols Re_τ = 2000-20000, y/δ 0.05

Lines ASL 600000, y/δ = 0.036

Further reading (i)

- Wyngaard, J. C. “Atmospheric turbulence” *Annu. Rev. Fluid Mech.* **24**: 205-33 (1992)
- Hogstrom, Hunt & Smedman *B. Layer Met.* **103:**101-124, 2002
- Metzger, Holmes & McKeon, “The near-neutral atmospheric surface layer: turbulence and non-stationarity” *Phil. Trans. Royal Soc. A* **365**: 859-876 (2007)
- Kunkel & Marusic, “Study of the near-wall-turbulent region of the high-Reynolds-number boundary layer using an atmospheric flow” *J. Fluid Mech.* **548**: 375-402 (2006)
- Guala, Metzger & McKeon, “Intermittency in the atmospheric surface layer: Unresolved or slowly varying?” *to appear, Phys. D. (2010)*
- Andreas et al “Evaluations of the von Karman constant in the atmospheric surface layer” *J. Fluid Mech.* **559**: 117-149 (2006)
- Hutchins & Marusic “Evidence of very long meandering features in the logarithmic region of turbulent boundary layers” *J. Fluid Mech.* **579**:1-28 (2007)
- Morris et al “Near-surface particle image velocimetry measurements in a transitionally rough-wall atmospheric boundary layer” *J. Fluid Mech.* (2007)

Summary

- Appears that near-neutral ASL can be used to get trend information for the structure of very high Reynolds number boundary layers.
- Several orders of magnitude gain in Re without usual problems of spatial resolution
- Still many difficulties associated with field tests
  - Practical
  - Convergence
  - “Outside influences”
- SLTEST demonstrated as good test site
- More work to be done…

Further reading (ii)

- Metzger & Klewicki, “A comparative study of near-wall turbulence in high and low Reynolds number boundary layers” *Phys. Fluids* **13**(3): 692-701 (2001)
- Mathis, Hutchins & Marusic “Large-scale amplitude modulation of the small-scale structures in turbulent boundary layers” *J. Fluid Mech.* **628**: 311-337 (2009)
- Guala, Metzger & McKeon “interactions within the turbulent boundary layer at high Reynolds number” *(submitted, 2009)*
- Marusic & Heuer “Reynolds number invariance of the structure inclination angle in wall turbulence” *Phys. Rev. Letters* **99**: 114504 (2007)
- J.R. Garratt “The Atmospheric Boundary Layer” *Cambridge University Press* (1992)
- J.L. Lumley & H.A. Panofsky “The Structure of Atmospheric Turbulence” *InterScience* (1964)
- C.H.B. Priestley “Turbulent Transfer in the Lower Atmosphere” *University of Chicago Press* (1959)